Substrate entering and product leaving trajectories predict an engulfing dynamic for the major conformational change of the β-lactam acylase

Xi Huang[1*], Jun Yin[1], Weihong Jiang[2], Zixin Deng[1], Guo-ping Zhao[2*]

1. Laboratory of Microbial Metabolism and School of Life Science and Biotechnology, Shanghai Jiaotong University, Shanghai 200030, China,

2. Shanghai Institute of Plant Physiology and Ecology, Shanghai Institutes for Biological Sciences, The Chinese Academy of Sciences, 300 Fenglin Road, Shanghai, 200032 China.

It is still a major challenge to acquire insight into the conformational changes between the ground state and the transition state of an enzyme, although conformational fluctuation within interconverting conformers has been widely investigated [1-4]. Here, we utilize different enzymatic reactions in β-lactam acylase to figure out the substrate/product trajectories in the enzyme, thereby probing the overall conformational changes in transition state. First, an auto-proteolytic intermediate of cephalosporin acylase (EC 3.5.1.11) with partial spacer segment was identified. As a final proteolytic step, the deletion of this spacer segment was revealed to be a first-order reaction, suggesting an intramolecular Ntn mechanism for the auto-proteolysis. Accordingly, the different proteolytic sites in the acylase precursor indicate a substrate entering pathway along the spacer peptide. Second, bromoacyl-7ACA can interact with penicillin G acylase (EC 3.5.1.11) in two distinguish aspects, to be hydrolyzed as a substrate analogue and to affinity alkylate the conserved Trpβ4 as a product analogue. The kinetic correlation between these two reactions suggests a channel opening from Serβ1 to Trpβ4, responsible for the main product leaving. These two reaction trajectories relaying

at the active centre, together with the crystal structures [5-10], predict an engulfing dynamic involving pocket constriction and channel opening.

Two comparable N-terminal nucleophile (Ntn) hydrolases [11,12], cephalosporin acylase (CA) and penicillin G acylase (PA) catalyze glutaryl-7ACA and penicillin G to produce 6APA and 7ACA respectively. Besides the normal substrate hydrolysis, the auto-proteolysis[13] of the spacer peptide in the pocket and the affinity alkylation [14] on the Trpβ4 in the tightly packed αββα motif (Fig. 1) would indicate the substrate entering and product leaving pathway in the enzyme.

Due to the lacking of sufficient knowledge concerning conformational dynamics, the question of how β-lactam acylases perform the auto-proteolysis has been discussed for years but remains a vigorous debate. It is unambiguous that the first auto-proteolytic step for both precursors is performed by an intramolecular interaction with the nucleophilic attack from the Oγ on the adjacent Serβ1[15-20]. However, it is unlikely that the following step(s) for the free spacer deletion adopt either the proposed intermolecular Ntn mechanism [16,17] or the intramolecular interaction with Gluα161 as nucleophile that was speculated from the spacer peptide with 9 amino acid residues [21], because CA has no effects on the removal of the free spacer peptide of its mutant [21] and the length of CA spacer is still uncertain [13,16,21]

To clarify the auto-proteolytic mechanism, an important auto-proteolytic intermediate of CA was investigated. With signal peptide removed [22], the CA from *p*KKCA1 often contains two different α-subunits as seen in previous SDS/PAGE [13] and MALDI-TOF spectrum [14]. The smaller one is a normal α-subunit (CAα), whose sequence is TPQ…RTLGE as determined by the MALDI-TOF spectra (Supplementary Fig. 1) and the MS/MS spectrum of its C-terminal trypic fragment TLGE (Supplementary Fig. 2). This confirms that the spacer peptide in this study is consisted

of 10 amino-acid residues, GDPPDLADQG [13]. The larger one, CAIα, whose sequence was determined as TPQ…RTLGE-GDPP (Supplementary Fig. 1), is the α-subunit of CAI, an important auto-proteolytic intermediate. It is possible that CAIα is generated *via* a two-step auto-proteolysis from the precursor in the periplasm. The first step involved is responsible for the cleavage of the peptide bond between Gly(-1) and Serβ1, generating the nascent α-subunit, followed by removal of the C-terminal segment DLADQG. The final step would encompass the *in vitro* removal of the remaining GDPP in order to generate CAα. To imitate the hydrolysis of the spacer peptide, a peptide analog, glutaryl-glutathione (GL-GSH) was synthesized. It can be hydrolyzed to produce glutathione (GSH) as main product (Supplementary Table 1; Supplementary Fig. 3). The latter can subsequently be hydrolyzed to produce Cys-Gly at a lower rate due to the weaker specificity of its side chain. Thus, the enzyme precursor is eligible to remove GDPP, DLADQG even GDPPDLADQG by one step.

Retaining the GDPP segment, CAI's catalytic activity decreased about 3-fold as estimated from the MALDI-TOF spectrum, so that the kinetics of the final auto-proteolytic step was followed by measuring the V_{max} of the CA mixture generated by incubation of CAI. It is important to note that the time-course of V_{max} of the enzyme at varying concentration fits to a single exponential equation which denotes a first-order process with $k_{obs} = 0.017$ min^{-1} (Fig. 2). Surprisingly, the rate of this auto-proteolysis can be enhanced significantly in the presence of 7ACA, which is a reversible inhibitor for the hydrolysis of GL-7ACA [23]. However, the reversible inhibition by glutaryl acid and the irreversible inhibition by bromoacyl-7ACA (BA-7ACA) alkylation were still seen on this auto-proteolytic step as expected (Fig. 2; Supplementary Fig. 1c).

These findings reveal an intramolecular Ntn mechanism for the auto-proteolysis, in which the specific side-chain binding interaction for normal substrate hydrolysis may not be essential, but the spacer "side-chain" that is already covalently bond to the α-

subunit C-terminus accounts for the deletion of the spacer GDPPDLADQG, DLADQG, GDPP or other spacer fragments with varying length as reported, ranging from 8-11 residues long [13,16,21,24]. This mechanism similarity between the auto-proteolysis and normal substrate hydrolysis can be enhanced by the mutagenesis study on both of the acylases with Serβ1 replaced by Cys. For PA, the mutant PA-Sβ1C can process as normal [25] with detectable hydrolytic activity (Supplemental Table 2). Without detectable hydrolytic activity, the mutant CA-Sβ1C can only perform the first auto-proteolytic step [17]. Accordingly, the different proteolytic sites figure out a substrate entering pathway along the spacer peptide from Gluα161 to Serβ1 and the measured distance of 21.54Å existing between Gluα161 and Serβ1 in the crystal structure (Fig. 1a) implicates a large scale conformational constriction tracked by the moving spacer peptide in the pocket. Although it is possible that the auto-proteolysis of PA contains a higher degree of complication due to the long spacer consisted of 54-amino-acid [9], the belief is held that PA would, at least partially, take on the same role.

It is not of unique nature that BA-7ACA and bromopropionyl-7ACA are able to inhibit CA *via* affinity alkylation of the non-solvent accessible Trpβ4 in the β-strand I [14]. Besides these two chemicals, bromoacyl-6APA can also affinity alkylate the conserved Trpβ4 of PA (Table 1; Supplementary Fig. 4). Furthermore, significantly inactivated mutant PA-Serβ1C can also be alkylated by BA-7ACA (Supplementary Table 2). The affinity alkylation site in PA was confirmed by the tandem MS spectrum of the related tryptic fragment from the PA labelled with BA-7ACA (Supplementary Fig. 5). The mutants with Trpβ4 replaced by Gly, His and Tyr were deprived of this alkylation (Supplementary Table 2).

Due to the hydrophobic side chain binding specificity, all the inhibitors with bromide side-chain can be hydrolyzed by PA as substrate analogs. Interestingly, the disassociation constant (K_i) of an affinity modification is very close to the respective

Michaelis-Menten constant (K_m) of hydrolyses, even when changing the reaction temperature (Table 1). Like the reversible competitive inhibition of PA by hydrolytic products [12], the side chain product PAA can protect PA from the alkylation in a competitive way, giving a disassociation constant (K_{PPA}') for the protection. Both observed K_m and K_i of BA-7ACA were increased on the same scale in the presence of PAA with different concentrations, concluding that $K_{PPA}=K_{PPA}$' (Fig. 3).

This existing correlation between the two enzymatic reactions can be interpreted as, after the main binding interaction, partial inhibitor was hydrolyzed as a substrate analog and the un-hydrolyzed inhibitor then became a β-lactam analog moving toward the Trpβ4 for alkylation [14]. Together with the crystal structure of PA (Fig. 1), this result suggests that in the conformational transition, a channel opening must occur between Serβ1 and Trpβ4 in the tightly packed αββα motif, involving in the substrate binding and the main product leaving, thereby allowing the bromide side-chain to alkylate the Trpβ4 after a movement of 15.23Å from side chain binding site (Fig. 1b).

Dynamic substrate binding with the participation of a channel can be substantiated by several observations on both PA and CA. Firstly, the substrate side chain is highly specific for both acylases, but the substrate's core can vary from -NH_2 to small peptide moieties (ref. 26, 27) (Table 1, Supplementary Fig. 4), so that the substrate-enzyme complex may only reflect the initial stage of substrate binding in ground state, which is dominated by side chain binding interaction [7]. Secondly, a little adjustment on the β2 by replacing Asnβ2 with Gln increased the K_m by 5-fold and decreased the k_{cat} by 10-fold [28]. Thirdly, the inhibitors entering the channel of PA are likely lead by the β-lactam moiety, subject to the hydrophobic side-chain binding interaction and the β-lactam moiety specificity for alkylation (Table 1). Lacking such side chain binding interaction in CA, the binding site for BA-7ACA alkylation may slip towards the Trpβ4 from the active centre, resulting in the significant decrease of the binding constant for

the mutant Wβ4Y [14]. Taking the β-lactam moiety as a C-terminal amino residue, this putative direction of the moving substrate is in accordance with that of the spacer peptide or the β-strand I, which can also be taken as a substrate's core in the first auto-proteolytic step. Lastly, unlike the metal chelation with EDTA, the dissociation constant for the reversible inhibition of PA with PAA (K_{PAA}) varies in the presence of differing substrate, ranging from 0.16 to 1.25 mM (Table 1). This variation may be subject to the capability for the substrate inducing the conformational change, reflecting that the side chain binding is likely to stabilize the ground state conformation. However, the dissociation constant of 6APA (K_{6APA}) remains almost unchanged (Table 1), implying the β-lactam's structural domination in the induction process.

The β-lactam structure induced transitional channel is unlikely to end at Trpβ4 but pass through the αββα motif along the β-strand I, allowing the alkylations on the β4 where besides Trp, Tyr [14] and Cys (unpublished data) were found to be alkylation targets in CA. The alkylation on Trpβ4 simultaneously inactivated the auto-proteolysis (Supplementary Fig. 1c) and the substrate hydrolysis, suggesting an integral channel required for the hydrolysis of the substrate with long chain, such as spacer peptides and GL-GSH. Since the alkylation occurs after hydrolytic reaction, suffering from the conformational recovery [14] whereby the binding for alkylation is less embodied in the K_i value, neither stopping at Trpβ4 nor going back to the pocket are likely actions of the leaving product. Interestingly, incomplete conformational recovery of the alkylated CA finally resulted in the slow hydrolysis of the inhibitor residue during the crystallization [29]. Accordingly, the unexpected rate enhancement experiment can be interpreted as a mechanism whereby 7ACA enters the induced channel compensating the energy required for the pocket constriction, and then rapidly passes the one-way channel rendering the space for GDPP leaving.

In conclusion, the intimately correlated different enzymatic reactions reveal the substrate entering and product leaving pathways in the acylases. These two relational trajectories, together with the crystal structures, predict a dynamic substrate binding interaction and an engulfing dynamic with large scale conformational changes both in the enzyme pocket and the αββα motif. The observing molecular movement of RNA by a nuclear magnetic resonance (NMR) technique [30] or fluorescence resonance energy transfer (FRET) [31] would be expected to interpret these dynamic events involving in the significant domain motions in the conformational transition. Under such a conformational dynamic, the energy released from the conformational recovery is likely to be a driving force for the next turn over. This molecular catalytic model offers an explanation for the major conformational change between ground state and transition state, which would be intended to be a motor-like energy transfer cycle for the catalysis.

Methods Summary.

Plasmid *p*KKCA1 [14] coding for CA (*acy*) was used for the expression of CAI. Plasmid pDB3 [32] carrying the gene coding for PA (*acy*) was used for expression of PA and the site-directed mutagenesis. The mutants of PA, PA-Wβ4A, PA-Wβ4H, and PA-Wβ4Y were constructed by a two-stage PCR method [32]. The auto-proteolytic kinetics of this intermediate was followed by measuring the increasing V_{max} of the CA mixture generated by incubating CAI at 37ºC in sodium phosphate buffer (pH 8.0). Alkylation of PA was carried out by incubating the acylase with BA-7-ACA in sodium phosphate buffer (pH 7.2) at 30°C. Steady-state kinetic parameters were determined from Lineweaver-Burk plots for the substrate hydrolysis or the double reciprocal plot for the affinity alkylation. MALDI-TOF Mass Spectrometric experiments on determination of CA α-subunits were performed on a Bruker REFLEX mass spectrometer as described [14]. On-line HPLC separation was performed on an Agilent 1100 LC-MS system for the MS-MS analysis of oligopeptide (see Methods).

References:

1. Alper, K. O., Singla, M., Stone, J. L. & Bagdassarian, C. K. Correlated conformational fluctuations during enzymatic catalysis: Implications for catalytic rate enhancement. *Protein Science* 10, 1319-1330 (2001).

2. Hammes, G. G. Multiple conformational changes in enzyme catalysis. *Biochemistry* 41, 8221-8228 (2002).

3. Eisenmesser, E. Z., Boco, D. A., Akke, M., and Kern, D. Enzyme dynamics during catalysis. *Science* 295, 1520-1523 (2002).

4. Whitten, S. T., Garcı´a-Moreno, E., & Hilser, V. J. Local conformational fluctuations can modulate the coupling between proton binding and global structural transitions in proteins, *Proc. Natl. Acad. Sci. U. S. A.*102, 4282–4287 (2005).

5. Kim, Y., Yoon, K. H., Khang, Y., Turley, S. & Hol, W. G. The 2.0 A crystal structure of cephalosporin acylase. *Structure* 8, 1059-1068 (2000).

6. Kim, Y., Kim, S., Earnest, T. N. & Hol, W.G. Precursor structure of cephalosporin acylase: insights into autoproteolytic activation in a new N-terminal hydrolase family. *J. Biol. Chem.* 277, 2823-2829 (2002).

7. Kim, Y. & Hol, W. G. Structure of cephalosporin acylase in complex with glutaryl-7-aminocephalosporanic acid and glutarate: insight into the basis of its substrate specificity. *Chem. Biol.* 8, 1253-64 (2001).

8. Duggleby, H. J., Tolley, S. P., Hil,l C. H. P., Dodson, E. J., Dodson, G. G. Y. Moody, P. C. E. (1995). Penicillin acylase has a single-amino-acid catalytic centre. *Nature* 373: 264-268

9. Hewitt, L., Kasche, V., Lummer, K., Lewis, R. J., Murshudov, G. N., Verma, C. S., Dodson, G. G. & Wilson, K. S. Structure of a slow processing precursor penicillin

acylase from *Escherichia coli* reveals the linker peptide blocking the active-site cleft. *J. Mol. Biol.* 302, 887-898 (2000).

10. Alkema, W. B., Hensgens, C. M., Kroezinga, E. H., de Vries, E., Floris, R., van der Laan, J. M., Dijkstra, B. W. & Janssen, D. B. Characterization of the β-lactam binding site of penicillin acylase of *Escherichia coli* by structural and site-directed mutagenesis studies. *Protein Eng.* 13, 857-863 (2000).

11. Brannigan, J. A., Dodson, G., Duggleby, H. J., Moody, P. C. E., Smith, J. L., Tomchick, D. R., & Murzin, A. G. A protein catalytic framework with an N-terminal nucleophile is capable of self-activation. *Nature* 378: 416-419 (1995).

12. Murzin, A. G., Brenner, S. E., Hubbard, T. & Chothia, C. SCOP: a structural classification of protein database for the investigation of sequences and structures. *J. Mol. Biol.* 247, 536-540 (1995).

13. Li, Y., Chen, J. Jiang, W. Xiang, M., Zhao, G., & Wang, E. *In vivo* post-translational processing and subunit reconstitution of cephalosporin acylase from *Pseudomonas* sp. 130. *Eur. J. Biochem.* 262, 713-719 (1999)

14. Huang, X., Zeng, R., Ding, X., Mao, X., Ding, Y., Rao, Z., Xie, Y., Jiang, W. H. & Zhao, G. P. Affinity alkylation of the Trp-B4 residue of the beta-subunit of the glutaryl 7-aminocephalosporanic acid acylase of *Pseudomonas* sp. 130. *J. Biol. Chem.* 277, 10256-10264 (2002).

15. Guo, H. C., Xu, Q., Buckley, D. & Guan, C. Crystal structure of flavobacterium glycosylasparaginase - an N-terminal nucleophile hydrolase activated by intramolecular proteolysis. *J. Biol. Chem.* 273, 20205-20212 (1998).

16. Kim, J. K., Yang, I. S., Rhee, S., Dauter, Z., Lee, Y.S., Park, S. S. & Kim, K. H. Crystal structures of glutaryl 7-aminocephalosporanic acid acylase: insight into autoproteolytic activation. *Biochemistry* 42, 4084-4093 (2003)

17. Lee, Y. S., & Park, S. S. Two-step autocatalytic processing of the glutaryl 7-aminocephalosporanic acid acylase from *Pseudomonas* sp. strain GK16. *J. Bacteriol.* 180, 4576–4582 (1998).

18. Lee, Y. S., Kim, H. W. & Park, S. S. The role of alpha-amino group of the N-terminal serine of beta subunit for enzyme catalysis and autoproteolytic activation of glutaryl 7-aminocephalosporanic acid acylase. *J Biol Chem.* 275, 39200-39206 (2000).

19. Kasche, V., Lummer, K., Nurk, A., Piotraschke, E., Rieks, A., Stoeva, S. & Voelter, W. Intramolecular autoproteolysis initiates the maturation of penicillin amidase from *Escherichia coli*. *Biochim. Biophys. Acta* 1433, 76-86 (1999).

20. Kim, S., & Kim, Y. Active site residues of cephalosporin acylase are critical not only for enzymatic catalysis but also for post-translational modification. *J. Biol. Chem.*, 276, 48376-48381 (2001).

21. Kim, J. K., Yang, I. S., Shin, H. J., Cho, K. J., Ryu, E. K., Kim, S. H., Park, S. S., Kim, K. H. Insight into autoproteolytic activation from the structure of cephalosporin acylase: a protein with two proteolytic chemistries, *Proc. Natl. Acad. Sci. U. S. A.* 103, 1732-1737 (2006).

22. Li, Y., Jiang, W., Yang, Y., Zhao, G., Wang, E. Overproduction and purification of glutaryl 7-aminocephalosporanic acid acylase. *Protein Expr. Purif.* 12, 233-238 (1998).

23. Aramori, I., Fukagawa, M., Tsumura, M., Iwami, M., Ono, H., Ishitani, Y., Kojo, H., Kohsaka, M., Ueda, Y., & Imanaka, H. Comparative characterization of new glutaryl 7-ACA and Cephalosporin C acylases. *J. Fermemt. Bioeng.* 73. 185-192 (1992).

24. Ishii, Y., Saito, Y., Fujimura, T., Isogai, T., Kojo, H., Yamashita, M., Niwa, M. & Kohsaka, M. A novel 7-β-(4-carboxy butanamido)cephalosporanic acid acylase

isolated from *Pseudomonas* strain C427 and its high-level production in *Escherichia coli*. *J. Ferment. Bioeng.* 77, 591-597 (1994).

25. Choi, K. S., J. A. Kim, and H. S. Kang. Effects of site-directed mutations on processing and activities of penicillin G acylase from *Escherichia coli* ATCC 11105. *J. Bacteriol*. 174: 6270-6276 (1992).

26. Huang, H. T., Seto, T. A. & Shull, G. M. Distribution and substrate specificity of benzylpenicillin acylase. *Appl. Microbiol.* 11, 1-6 (1963).

27. Alkema, W. B., Dijkhuis, A. -J., de Vries, E., & Janssen, D. B. The role of hydrophobic active-site residues in substrate specificity and acyl transfer activity of penicillin acylase. *Eur. J. Biochem.* 269, 2093-2100 (2002).

28. Zhang, N., Ding, X.M., Huang, X., Wang, E.D., Yang, Y.L., Zhao, G.P. & Jiang, W.H. Mutagenesis of N-terminal Amino Acid Residues in beta-subunit of Glutaryl-7-amino-cephalosporanic Acid Acylase C130. *Acta Biochi. Biophys. Sinica* 33, 671-676 (2001).

29. Zhang, W., Huang, X,. Zhao, G., & Jiang, W. Affinity labelled glutaryl-7-amino cephalosporanic acid acylase C130 can hydrolyze the inhibitor during crystallization. *Biochem. Biophys. Res. Commun.* 313, 555-558 (2004).

30. Zhang, Q., Stelzer, A. C., Fisher, C. K. & Al-Hashimi, H. M. Visualizing spatially correlated dynamics that directs RNA conformational transitions. *Nature* 450, 1263-1267 (2007).

31. Gondert, M. E., Tinsley, R. A., Rueda, D., & Walter, N. G. Catalytic core structure of the trans-acting HDV ribozyme is subtly influenced by sequence variation outside the Core. *Biochemistry* 45, 7563-7573 (2006).

32. Dai, M. H., Wang, E. D., Xie, Y., Jiang, W. H., Zhao, G.P. Site-directed mutagenesis of the active center of penicillin acylase from E. coli ATCC 11105. *Acta Biochi. Biophys. Sinica* 31, 558-562 (1999).

This work was funded by the National High Technology Development Program of China. The amino acid sequence of CA from Pseudomonas sp. 130 can be accessed through the NCBI Protein Database under NCBI Accession # 11386616. The atomic coordinates for the CA from Pseudomonas sp. 130 were deposited in the Protein Data Bank under accession number 1GHD.

Correspondence to: Xi Huang[1] or Guo-ping Zhao[2] Correspondence and requests for materials should be addressed to X. H. (Email: xhuang@sjtu.edu.cn) or G. –p. Z. (Email: gpzhao@sibs.ac.cn)

Figure legends

Figure 1. **Orthogonal view of the structures of CA (a, with atom background in line model) and PA (b) with the key residues related to different enzymatic reactions.** Protein backbone with α-subunit (in blue) and β-subunit (in brown) is shown as a completely flat ribbon. As there are no significant differences among the overall structures of precursor, matured acylase and enzyme-substrate complex for either CA or PA, the spacer peptide and substrate are superposed to illustrate the positions of auto-proteolytic sites and substrate. The spacer peptide and the first β-strand I, which is the N-terminal fragment of the β-subunit deposited in the first β-layer of the αββα motif, are shown in light or dark green sold ribbon. The light green colour represents the substrate amino residues (in stick model) and the spacer fragments (in sold

ribbon); the red colour in stick model represents the substrate side-chain, the Pro(-7) and Gluα161 that can be regarded as the spacer "side chain" covalently bond to α-subunit; the black colour in stick model represents the reaction sites indicated by the nucleophile Serβ1 and alkylation site Trpβ4. The distance between the Oγ of Serβ1 and carboxyl group of α-subunit C-terminal Gluα161 (dotted green line in CA, 21.54 Å) and the distance between the Cα of substrate side-chain and the Cδ of Trpβ4 (dotted green line in PA, 15.33 Å) were measured by software DS ViewerPro (Accelrys Co.).

Figure 2. **The auto-proteolytic kinetics of CAI and the activation/inactivation by the hydrolytic products of GL-7ACA/glutaryl acid.** The auto-proteolysis of CAI was carried out by adding the enzyme to the pre-incubated 100 mM sodium phosphate buffer (pH 8.0) with different concentrations of 7ACA (0.0, 0.5, 1.0 and 2.0 mM) and glutaryl acid (0.5, 1.0 and 2.0 mM) at 37ºC. In each time interval, aliquots were immediately added to 5.0 mM GL-7ACA (pH 8.0) for enzyme activity assay[14], in which the background of 7ACA was deducted by taking the immediately quenched reactions as controls. As the fraction of CA is lineally coupled with the increasing of the $V_{max,t}$ of the enzyme, the first order rate constant, *k*, was obtained by fitting the data to the equation $V_{\max,t} = V_0 + V_\infty(1 - e^{-kt})$, where $V_{max,t}$ is the V_{max} of the enzyme mixture at time *t*, V_0 is the initial V_{max} of the fresh CAI, V_∞ is the latitude. Data analysis and graph preparation were done with KaleidaGraph (Synergy Software, PA). The curve fitting program would not fit data obtained for the inactivation by glutaryl acid with concentration of 1.0 and 2.0 mM, unless the end point was fixed. Therefore, the end point was set to a reasonable, though somewhat arbitrary value. Three independent experiments were carried out with different initial enzyme concentrations of 0.2, 0.3 and 0.4 mg/ml.

Figure 3. Kinetic comparison between the deacylation of BA-7ACA in PA and the affinity alkylation of PA with BA-7ACA. The Lineweaver-Burk plots (●) of the deacylation of BA-7ACA by PA were carried out in the present of PAA with concentration of 0.0 mM (dark line), 0.25 mM (green line) and 0.5 mM (red line), giving the kinetic constants of K_m, k_{cat} and the disassociation constant K_{PAA} for the competitive inhibition caused by PAA. The loss of the enzyme activity of PA by affinity alkylation was assumed to proceed *via* a pseudo first-order reaction at initial stage and the rates of the inactivation (k) was plotted against different concentrations of BA-7ACA (3.6. 5.4, 8.1, 12.2 and 18.3 mM) in double reciprocal plot (▲, dark line), giving the disassociation constant K_i and the rate constant k_{max} (ref. 14). The protection of the alkylation kinetics employed the same procedures in the present of PAA with concentration of 0.25 (green line) and 0.50 mM (red line), giving the disassociation constant K_{PAA}' for the competitive protection. All the data given in the plots were mean of three independent experiments.

Table 1. Steady-state kinetic parameters of PA for hydrolyses and affinity alkylation.

Substrate	K_m (mM)	k_{cat} (s^{-1})	K_i (mM)	k_{max} (min^{-1})	K_{PAA} (mM)	K_{6APA} (mM)
m-BA-ABA	3.0	2.1	x	x	0.16	-
p-BA-ABA	2.1	0.80	x	x	0.17	-
BA-6APA	4.8	5.3	4.5	0.041	0.17	-
BA-7ACA	6.7/3.8*	7.2/7.9*	6.9/3.6*	0.19/0.22*	0.17	12.9
BP-7ACA	6.2	5.9	6.3	0.021	0.23	-
BB-7ACA	3.7	15.0	x	x	0.28	-

Bpental-7ACA	2.6	12.2	x	x	0.34	-
BH-7ACA	1.45	4.6	x	x	0.33	-
NIPAB	0.11	51	x	x	0.35	13.0
PG**	0.24	94	x	x	1.25	13.9

All parameters for the substrates (see Supplementary Fig. 4) were determined at 30ºC, except for "*". Values are means of at least three independent experiments and standard deviations are <10%, except for "**". "x": Undetectable. "-": not available. "*": Determined at 37ºC. "**": standard deviation is ~15%. The kinetic constants K_m and k_{cat} were determined from Lineweaver-Burk plots. Alkylation kinetic parameters (K_i and K_{max}) were obtained from the similar procedure by determined the loss of enzyme activity (see Methods). K_{PAA} and K_{6APA} was obtained by measuring the different apparent K_m's in the present of PAA with different concentrations of 0. 25 mM and 0.5 mM and 6APA with different concentrations of 0.5 mM and 1.0 mM.

Figure 1

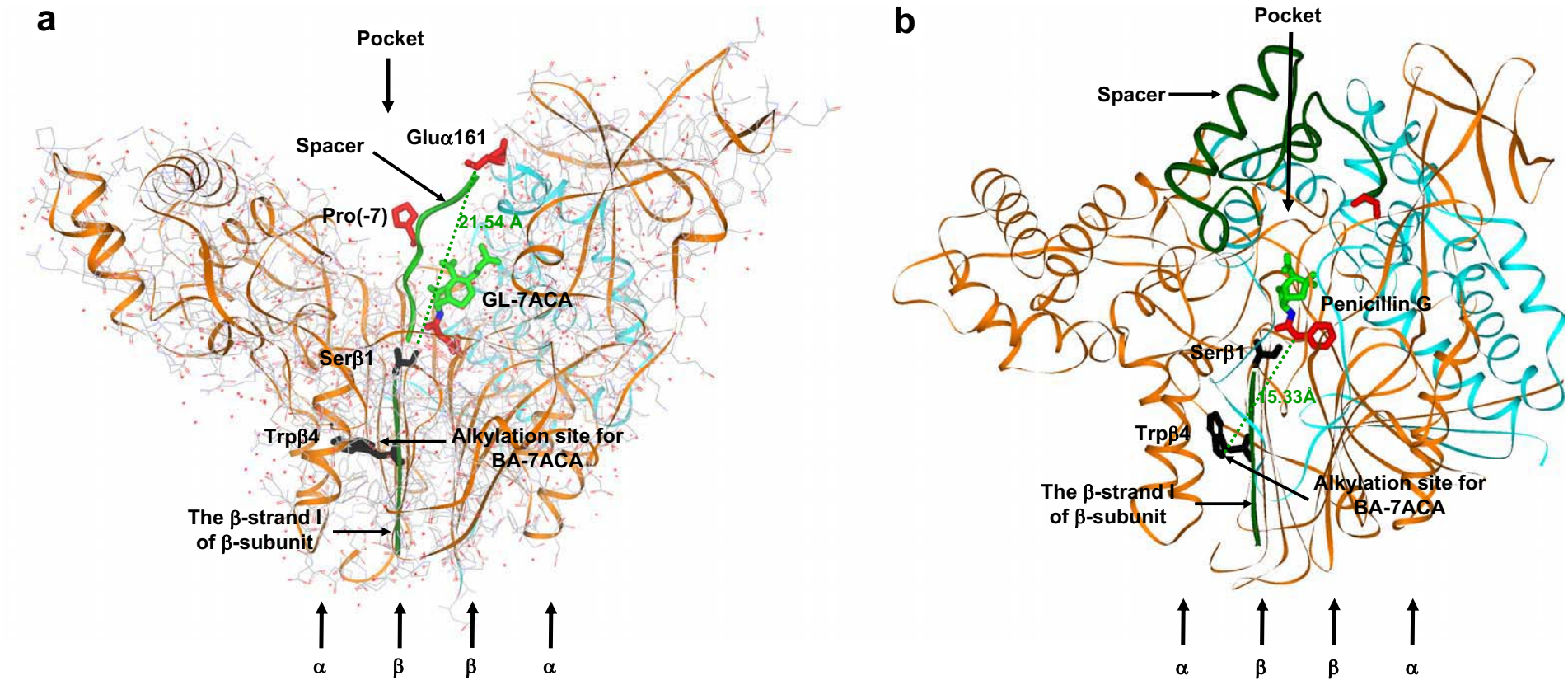
a
Pocket
Spacer
Gluα161
Pro(-7)
21.54 Å
GL-7ACA
Serβ1
Trpβ4
Alkylation site for
BA-7ACA
The β-strand I
of β-subunit
α
β
β
α
b
Pocket
Spacer
Penicillin G
Serβ1
15.33Å
Trpβ4
The β-strand I
of β-subunit
Alkylation site for
BA-7ACA
α
β
β
α

Figure 2

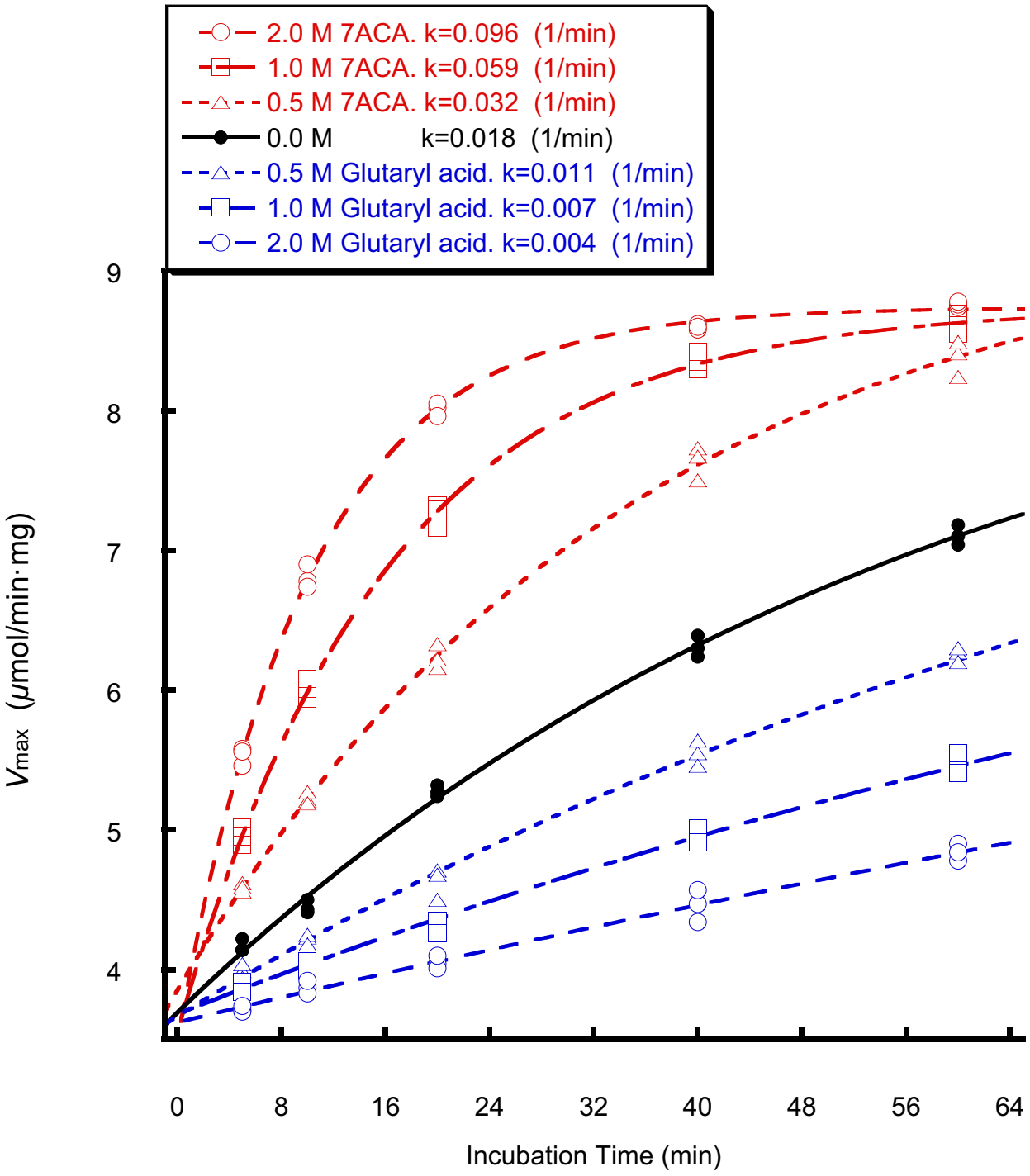
2.0 M 7ACA. k=0.096 (1/min)
1.0 M 7ACA. k=0.059 (1/min)
0.5 M 7ACA. k=0.032 (1/min)
0.0 M k=0.018 (1/min)
0.5 M Glutaryl acid. k=0.011 (1/min)
1.0 M Glutaryl acid. k=0.007 (1/min)
2.0 M Glutaryl acid. k=0.004 (1/min)
Vmax (μmol/min·mg)
9
8
7
6
5
4
0
8
16
24
32
40
48
56
64
Incubation Time (min)

Figure 3

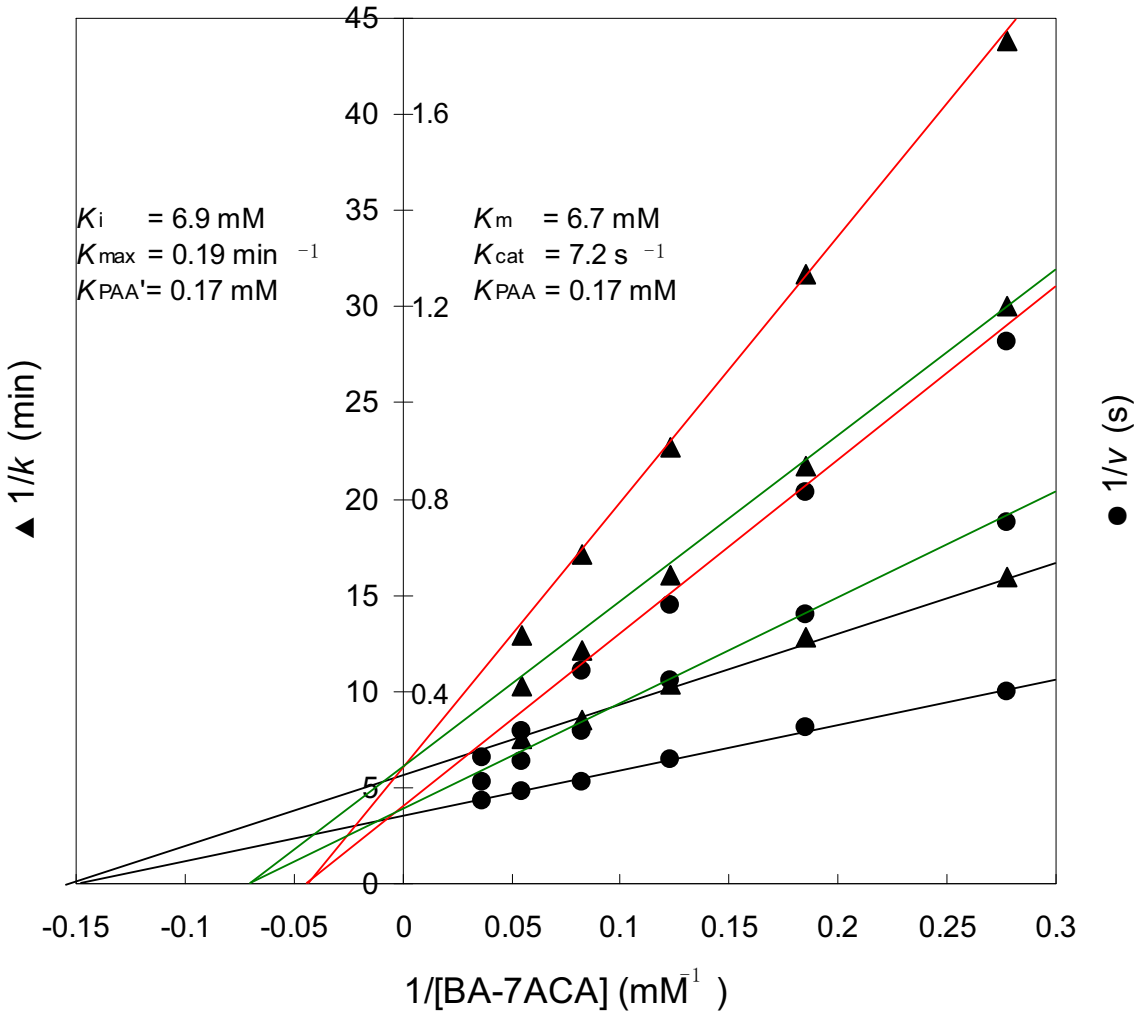
Ki = 6.9 mM
Kmax = 0.19 min −1
KPAA'= 0.17 mM
Km = 6.7 mM
Kcat = 7.2 s −1
KPAA = 0.17 mM
▲ 1/k (min)
● 1/v (s)
1/[BA-7ACA] (mM−1)
45
40
35
30
25
20
15
10
5
0
1.6
1.2
0.8
0.4
-0.15
-0.1
-0.05
0
0.05
0.1
0.15
0.2
0.25
0.3